ENVIRONMENTAL RESEARCH
COMMUNICATIONS

LETTER • OPEN ACCESS

Temporal and spatial assessment of gaseous elemental mercury concentrations and emissions at contaminated sites using active and passive measurements

To cite this article: David S McLagan *et al* 2021 *Environ. Res. Commun.* **3** 051004

Environmental Research Communications

LETTER

Temporal and spatial assessment of gaseous elemental mercury concentrations and emissions at contaminated sites using active and passive measurements

David S McLagan[1], **Stefan Osterwalder**[2] **and Harald Biester**[1]

[1] Department of Environmental Geochemistry, Institute for Geoecology, Technical University of Braunschweig, Braunschweig, Germany
[2] Department of Environmental Sciences, University of Basel, Basel, Switzerland

E-mail: d.mclagan@tu-braunschweig.de

Keywords: gaseous elemental mercury, active monitoring, passive sampling, emissions fluxes

Supplementary material for this article is available online

OPEN ACCESS

RECEIVED
27 January 2021

REVISED
12 April 2021

ACCEPTED FOR PUBLICATION
4 May 2021

PUBLISHED
12 May 2021

Abstract

Gaseous elemental mercury (GEM) concentrations and emissions at legacy contaminated sites represent poorly characterised components of global mercury (Hg) inventories. Here we apply both active (Tekran 2537A) and passive (MerPAS) sampling methods to comprehensively assess GEM concentrations and emissions across four dimensions (three spatial, one temporal) at a legacy contaminated site with elevated soil Hg. Concentrations are measured up to 37.4 (active) and 10.8 (passive) ng m^{-3}, which represents enhancements of 23× and 7× above background (1.62 ng m^{-3}), respectively. Temporal resolution of the sampling methods defines this difference (active: 5-min; passive: 44 days). Diurnal (active) GEM concentration patterns were highest in contaminated areas at night when low wind speeds compress the boundary layer. Passive sampling substantially improves the spatial characterisation of GEM concentrations both horizontally (highest GEM concentration in areas with elevated soil Hg) and vertically (improved vertical concentration gradient using telescopic sampling towers). Passive sampler deployments were used to generate a GEM emissions estimate (landfill-to-atmosphere) of 1.2 ± 0.6 kg yr^{-1} (or 310 ± 150 ng m^{-2} h^{-1}). This study demonstrates how combining active (strength: temporal assessment) and passive (strength: spatial assessments) sampling improves the evaluation of GEM concentrations and emissions to the atmosphere at Hg contaminated sites across four dimensions.

1. Introduction

It is essential that we characterise mercury (Hg) emissions to the atmosphere with constrained uncertainties as the atmosphere is the primary pathway for the global redistribution of Hg, a pollutant with considerable environmental and human health implications (UNEP 2013, Driscoll *et al* 2013). Sources of Hg emissions to the atmosphere are many and are spatially distributed across the world. These include both natural and anthropogenic sources. Typically, emission estimates of active anthropogenic sources (i.e. coal combustion, gold mining, and certain industrial processes) that contribute to national, continental, and global Hg inventories use a bottom-up approach based on end product production rates or Hg stock input data (Pacyna *et al* 2010, Pirrone *et al* 2010).

There are also 'legacy' emissions from sites contaminated by Hg containing waste materials, Hg use in processing, or Hg production. Contamination at many of these legacy sites is associated with Hg in soils and emissions to the atmosphere typically correlate with total Hg concentrations in these soils (Edwards *et al* 2001, Agnan *et al* 2016, Osterwalder *et al* 2019). Legacy site emissions are more difficult to define as they are often no longer related to a single point source (diffuse area sources) as production has ceased, meaning a bottom-up approach is not possible (Kocman *et al* 2013). Two main approaches exist for estimating emissions from such sites: (i) upscaling of *in situ* terrestrial substrate-to-atmosphere flux measurements (Engle *et al* 2001, Wang *et al*

2005), or (ii) top-down or inverse-modelling approaches based on atmospheric Hg concentration measurements (typically using active monitoring instruments or satellite spectra) that are elevated above background at these sites (Ferrara *et al* 1998, Song *et al* 2015). Nonetheless, these methods of emissions estimations have elevated uncertainties associated with the instrumentation, poor spatial distribution of sampling (limited instrument mobility: non-representative sampling), and non-concurrent measurements (introduce temporal concentration variability), (Kocman *et al* 2013, Zhu *et al* 2015, Agnan *et al* 2016, McLagan *et al* 2019).

Recently, McLagan *et al* (2019) presented a novel, top-down approach to characterise gaseous elemental Hg (GEM) concentrations and emissions (dominant form of Hg in the atmosphere and in emissions; Streets *et al* 2017, Tao *et al* 2017) at contaminated sites using a novel GEM passive air sampler (MerPAS). These sampling instruments are low-cost, easy-to-deploy, do not require electricity, and are able to produce highly precise and accurate GEM concentration data (McLagan *et al* 2016, 2017b, 2018a, Jeon *et al* 2020, Wohlgemuth *et al* 2020, Naccarato *et al* 2020). They can also be deployed concurrently and in high numbers (including vertical deployments) that allows unprecedented high spatial resolution characterisation of GEM in and around source sites (McLagan *et al* 2018b, 2019). However, the weakness of this method is the temporal resolution of the GEM concentrations produced. Data are time-averaged across the whole period in which they are deployed and cannot provide high-temporal resolution assessments of the variability in GEM concentrations and emissions (i.e. diurnal changes). Such measurements require high sampling resolution active monitoring instruments (i.e. Tekran 2537 series instruments; Tekran Instruments Corp); thus, both systems have their strengths and limitations.

This study examines GEM concentrations measured with MerPAS (passive) and Tekran 2537A (active) instruments in and around a legacy site contaminated with Hg-containing waste materials in Switzerland. These active and passive GEM concentration data assess diurnal changes and the variability across three-spatial dimensions (3D; vertical tower), respectively, as well as chronic inhalation exposure risks to the local population. Furthermore, the 3D MerPAS deployments are used to generate an emissions flux from the site based on the method developed by McLagan *et al* (2019).

2. Methods

2.1. Site description

The contaminated site is the Gamsenried landfill (total area $\approx$ 300000 m^2) that has had an estimated 3.0 $\times$ 10^6 m^3 of waste materials deposited from a nearby chemical plant, materials which contain an estimated 33 tonnes of Hg. Hg was used at the chemical plant predominantly in acetaldehyde, vinyl acetate, vinyl chloride, and chlor-alkali processing. Both the chemical plant and the landfill site are situated in the upper Valais in Switzerland between 650 and 700 m above sea level. The Rhone Valley runs approximately ENE to WSW at the site of the landfill and the wind regime (particularly in summer) is dominated by moderate ENE winds in the morning and moderate-to-strong WSW winds in the afternoon. The landfill site is divided up into sectors laid out in figure 1, which also contains both the active and passive sampling locations.

2.2. Active sampling methods

Active GEM concentrations measurements were made with a Tekran 2537A (Tekran Instruments Corp.). Details of the analytical setup of the Tekran 2537A and associated meteorology measurements (mounted on the same sampling tower) are detailed in section S1 (available online at stacks.iop.org/ERC/3/051004/mmedia). Although this system may sample some gaseous oxidised Hg, its contribution to total gaseous Hg is small (likely $<$5%) as GEM is the dominant form in the air and the most readily released from contaminated substrates (Lyman and Gustin 2008, Engle *et al* 2010, Kocman and Horvat 2011, O'Connor *et al* 2019). For terminology consistency with passive sampling data, we will also use GEM as the active measurement analyte. Uncertainty associated with this terminology is likely less than the estimated method uncertainty of the Tekran 2537 instruments (5%–10%; Aspmo *et al* 2005, Temme *et al* 2007).

Active measurements were made at four sites, three in the landfill area and one 250 m to the west (figure 1) in the summer of 2016. Site A1 is situated in Sector E1 and sampling was made from 15:00 CEST 21.07.2016 to 9:55 CEST 29.07.2016 (n = 2195). Nighttime was characterised by solar radiation of $<$5 W m^{-2}. Nighttime GEM concentrations represented 41% of the sampling period at site A1. Sampling at site A2 (at the juncture of Sectors F2, F3, H, and E) took place from 14:00 CEST 05.08.2016 to 7:50 16.08.2016 (n = 3006) and nighttime accounted for 42% of the measurements. Sampling at site A3 (Sector 3) occurred from 13:55 CEST 29.07.2016 to 10:30 CEST 05.08.2016 (n = 1934); nighttime accounted for 42% of data. Finally, site A4 was the site outside the landfill area (250 m to the west of Sector P), sampling took place from 16:00 CEST 16.08.2016 to 22:35 CEST 27.08.2016 (n = 3171) and nighttime represented 46% of the samples.

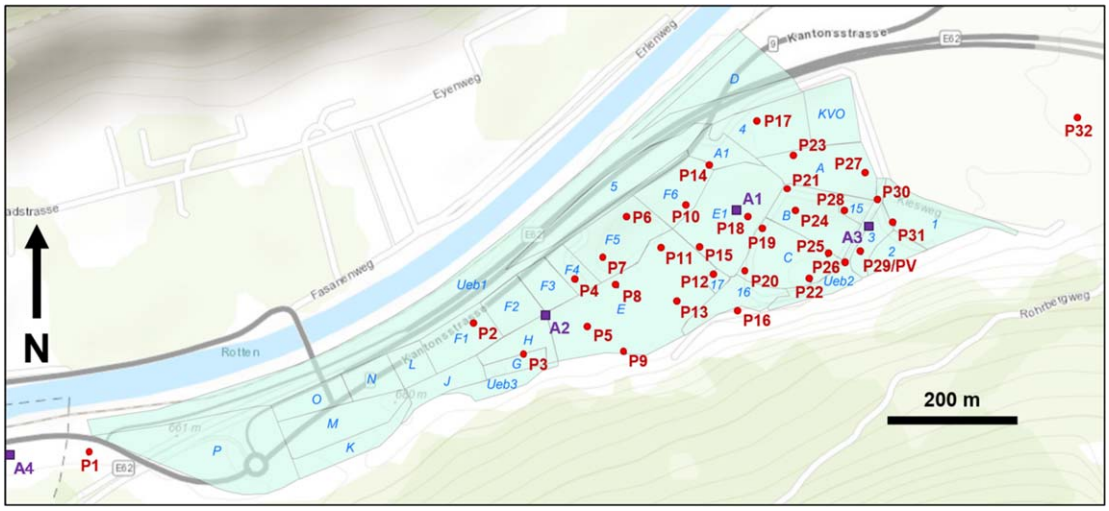

Figure 1. Map of Gamsenried landfill site showing landfill sectors (blue text), active (A1-A4; purple squares, purple text) and passive (P1-P32; red circles, red text) sampling sites. The vertical gradient tower is marked by P29/PV in Sector 3. Map created with ArcGIS (Esri).

2.3. Passive sampling methods

Passive GEM concentrations were measured with MerPAS, designed, and tested by researchers at the University of Toronto and now commercialised with Tekran Instruments Corp. Recent data have shown this passive sampler is the best available for GEM concentration monitoring (Naccarato *et al* 2020) and GEM to be the target analyte (Szponar *et al* 2020). The activated carbon sorbent was analysed for total Hg with a DMA80 (Milestone Instruments, Sorisole, Italy). Details of MerPAS, the analytical method, and concentration calculations are provided elsewhere (McLagan *et al* 2017a, 2018a). MerPAS sampling rate derivation and QA/QC data specific to this study are presented in section S2.

30 MerPAS were deployed at 1.5 m above-ground-level across the Gamsenried landfill site and an additional three background control sites, adjacent to the landfill site to the east and west and in the town of Visp (≈4 km to the west of the landfill), for ≈43 days in summer (07.07.2020–19.08.2020). The deployments were not evenly distributed across the whole landfill site, but rather concentrated in the eastern half of the site where total soil Hg concentrations are most elevated and elemental Hg (Hg°) is also present in some samples (Biester 2020; selected data included in section S3) and in areas in which the elevated GEM concentrations were measured in the earlier active sampling field campaign (this study). Additionally, the vertical GEM concentration gradient was also assessed using duplicated MerPAS deployed at 0.5, 2, 4, 6, 8, and 10 m on a telescopic sampling tower at site 29. This is a critical component of generating an emissions estimate of GEM from the site based on these MerPAS deployments. The 1.5 m GEM concentration used for the horizontal spatial assessment at site 29 was interpolated from the model of the measured vertical concentration gradient. MerPAS concentrations were geospatially interpolated using the same Bayesian log empirical kriging method applied in McLagan *et al* (2019). All maps and kriging variogram models were produced using ArcGIS 10.5.1 (Esri Ltd) and their details can be found in section S4.

2.4. Emissions estimate calculations

The emissions estimate is based on the method developed by McLagan *et al* (2019). Details can be found there, and a method outline is given in figure S4. However, some adjustments were made (this includes making the estimate at 0.5 m—the lowest sampling height of the vertical profile) and are described in section S4. A slightly more complex model was also evaluated. McLagan *et al* (2019) describe the importance of avoiding spatial imbalances in sampling, but also ensuring that measurements are made at all possible areas in which emissions may occur. Sample spacing was not even in this study to ensure areas where elevated soil Hg concentrations were sufficiently characterised. The more detailed model used the geospatially interpolated (Bayesian log empirical kriging) contours to remove spatial imbalance of the sampling sites. Details of this method are also outlined in section S4.

3. Results and discussion

3.1. Temporal variability of GEM concentrations

Temporal GEM concentration variability was monitored with 5-min resolution measurements taken by the Tekran 2537A at the four active sampling sites and these data are presented in figure 2 based on diurnal concentration variability and variability by wind speed (see section S5 for summary statistics and times series of active GEM concentration and meteorological data). During sunny days (clear skies) strong valley winds from the west (180°–360°) typically dominated between ≈11:00 and ≈20:00 (figure 2). GEM evasion from the landfill might be expected to be higher during the day because elevated solar radiation is reported to drive Hg flux (Carpi and Lindberg 1997, Poissant and Casimir 1998, Choi and Holsen 2009). However, this effect could not be directly observed in active GEM concentrations. GEM emissions were likely occurring, but the higher wind speeds during daytime act to advectively disperse these emissions by mixing locally emitted GEM with background GEM concentrations. The median nighttime GEM concentrations were a factor of 1.5× and 2.2× higher compared to daytime values for sites A1 and A2, respectively. Elevated GEM concentrations at sites A1 and A2 were associated with low wind velocities, low air temperatures, high relative humidity and low atmospheric pressure. Statistical correlation between Hg concentration and these variables were significant ($p < 0.05$, see section S5 for details). Nighttime conditions at these sites indicated weak mixing of air masses and accumulation of Hg in the compressed nocturnal boundary layer (figure 2).

At site A3, mean daytime and nighttime GEM concentrations were 2.9 ± 1.8 ng m^{-3} and 2.7 ± 1.3 ng m^{-3}, respectively. This is in contrast to sites A1 and A2 in which GEM building up in the nocturnal boundary layer was the main process controlling this temporal GEM concentration variability. GEM concentrations typically peaked during periods of westerly winds often after sunrise (figure 2) and were above 3 ng m^{-3} for 35% during westerly winds. Advection of air masses from the eastern end of the landfill contained lower GEM concentrations, exceeding 3 ng m^{-3} only 12% of the time. During the night, advection of air masses with lower GEM from outside the landfill in the east, might have hampered build-up of elevated GEM above the surface (easterly wind direction occurred in 54% of the time). This is demonstrated by GEM concentrations of 2.2 ± 0.8 ng m^{-3} measured during periods of easterly and 3.2 ± 1.6 ng m^{-3} during periods of westerly winds. Statistical correlation at site A3 between GEM concentration and meteorological variables were weak ($r < 0.2$). Weak negative correlations between daytime GEM concentrations and solar radiation at all sites implied efficient mixing of ambient GEM that likely outweighed any effect of solar radiation on releases of GEM from soils.

Sampling at site A4 (site to west of landfill) was divided into two distinct periods based on the activity of the municipal waste incineration plant situated in Sector KVO of the landfill: (i) incineration plant idle (16:00 16.08.2016 to 0:00 24.08.2016), and (ii) incineration plant active (0:05 24.08.2016 to 22:35 27.08.2016). The GEM concentration measured when the waste incineration plant was in idle mode during easterly and westerly winds exceeded the threshold of 3 ng m^{-3} in only 0.5% and 1.5% of the time, respectively (Section S5.4). Diurnal cycles of GEM concentrations were less pronounced at this location during the idle period compared to the sampling sites A1, A2 and A3 located on the landfill (figure 2). This is typical for concentration measurements at uncontaminated sites with no Hg point sources in the fetch. Thus, this location was utilised to determine the regional background (1.62 ng m^{-3}), which was calculated as the median value of the data during 87 h of measurements during westerly winds at A4 when the incineration plant was idle. This concentration is in line with measurements of background Hg concentrations in the Northern Hemisphere, and in particular with another monitoring station in the European Alps (Col Margherita, Italy) whose median GEM concentration during 2014 was 1.65 ng m^{-3} (Sprovieri *et al* 2016).

When the incineration plant was in operation GEM concentrations at site A4 increased by about 10%, the proportion of GEM concentrations above 3 ng m^{-3} during this period increased to 12%, and showed a distinct midday concentration peak, although this peak gradually decreased from August 24 to August 27 (Section S5.4). Furthermore, the average concentrations advected from the east, increased from 1.7 to 1.9 ng m^{-3}. Thus, it is likely that GEM concentrations were affected by the restart of the municipal waste incineration plant. Interestingly, average GEM concentrations in air masses from the west also increased from 1.8 and 2.2 ng m^{-3}. Trends between GEM concentrations and meteorological parameters also differed. During plant downtime GEM concentrations decreased with increasing wind speed, air temperature, solar radiation, and atmospheric pressure (section S5.4). In contrast, when operation restarted, correlations between GEM concentration, air temperature and solar radiation were positive (section S5.3). This may be related to GEM emissions from the elevated stack height of the incineration plant remaining in the valley; emissions are blown to the west by morning easterlies and then return to the area when the winds reverse direction from the late morning.

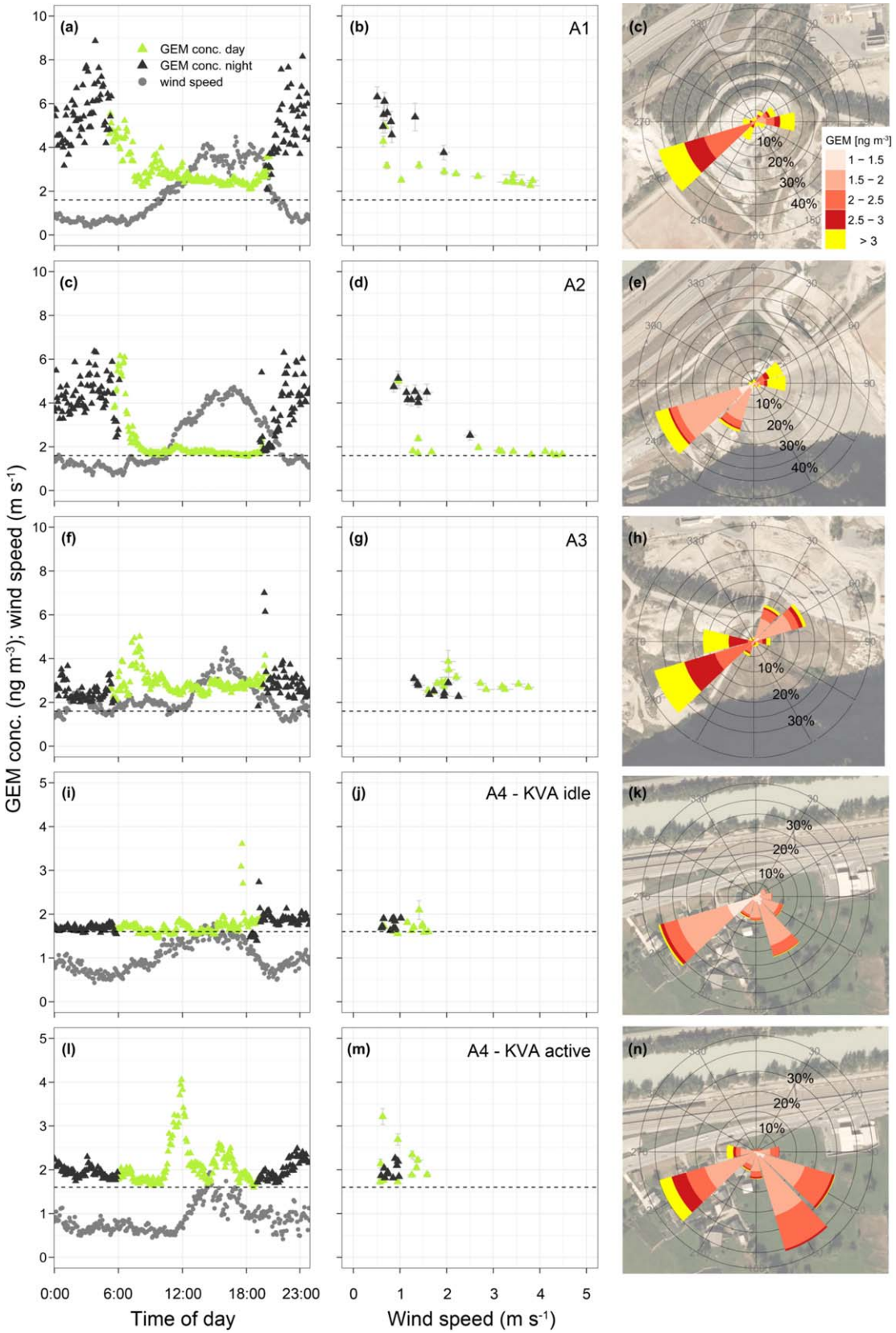

Figure 2. Left panels: Diurnal mean 5-min GEM concentrations and wind speeds for each active monitoring site (green triangles—day; black triangles—night; grey dots—wind speed). Centre panels: mean hourly mean GEM concentration variability by wind speed. Right Panels: wind rose graphs indicating proportion of pooled active GEM concentrations. KVA represents waste incineration plant.

3.2. Spatial variability of GEM concentrations

The time-averaged GEM concentrations measured using MerPAS ranged from 1.22 ng m^{-3} at site P30 (Sector 1) up to 10.8 ng m^{-3} at site P20 (Sector C), the latter of which is an enhancement by a factor of ≈9 above

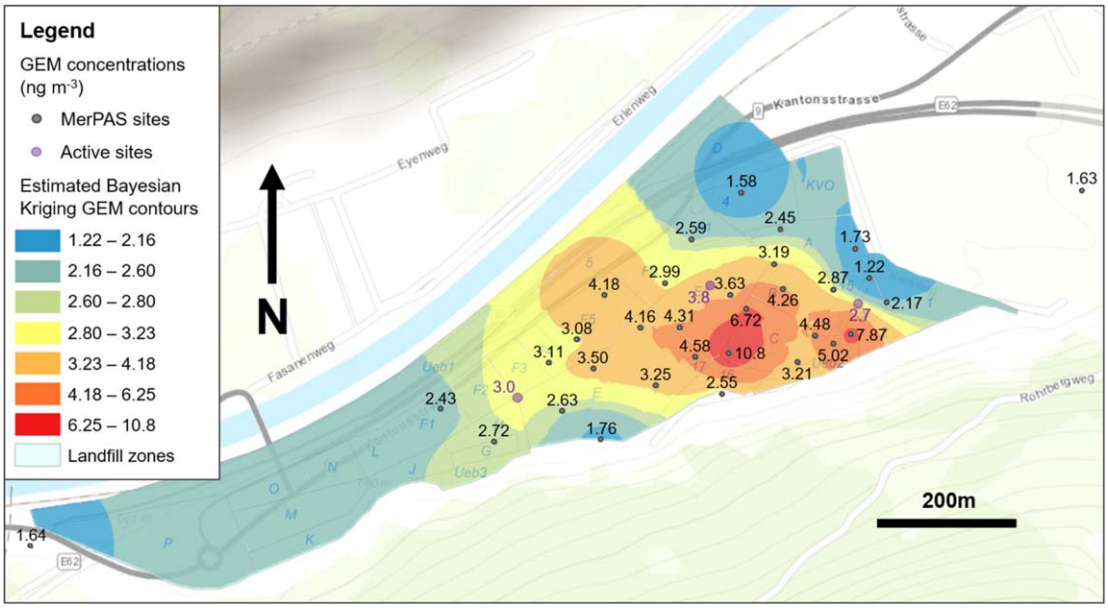

Figure 3. Measured (MerPAS) and geospatially interpolated (Bayesian log empirical kriging) GEM concentrations across the Gamsenried landfill site. Mean measured GEM concentrations from active measurements at sites A1, A2, and A3 are included in this map (purple text). Map created with ArcGIS (Esri).

background (figure 3; section S6). These passively derived GEM concentrations were geospatially interpolated using log empirical Bayesian Kriging to enhance the visualisation of the spatial distributions of concentrations (figure 3). Highest GEM concentrations were observed in landfill Sectors C and 3 which agrees with previous assessments of total soil Hg concentrations that were elevated in Sectors 3 and C in particular (Steinmann, 2016, Biester, 2020). Furthermore, the presence of unbound Hg° was detected above depths of 2 m in several soil cores in Sectors 3 and C using pyrolytic thermal desorption (Biester 2020; data included in section S3). Considering the high volatility of Hg°, gas phase partitioning of unbound Hg° in landfill soils is likely to contribute to the elevated GEM concentrations across the site. Photoreduction of Hg^{2+} to Hg° in soils and subsequent partitioning to the gas phase may also contribute to the elevated GEM concentrations we observed in these sectors of the Gamsenried landfill site (Gustin *et al* 2002, Choi and Holsen, 2009, Carmona *et al* 2013). There seems to be little influence from any Hg emissions from the municipal waste incinerations plant on GEM concentrations measured at adjacent MerPAS sites likely due to the height of releases from the emissions stack of the facility.

The maximum active GEM concentrations measured by the Tekran 2537A (up to 37.4 ng m^{-3} site A1; see section S5 for details) were distinctly higher than the MerPAS concentrations. However, the Tekran 2537A provides much higher temporal resolution data than MerPAS and can identify short term variability in concentrations. Thus, it is more appropriate to compare mean active concentrations to the MerPAS data. When we consider the mean values measured at the four active sampling sites, similarities between the GEM concentrations of the two methods are more apparent. The highest mean GEM concentration measured was at A1 (3.8 ng m^{-3}), adjacent to MerPAS site P18 (3.63 ng m^{-3}), and the concentrations were essentially analogous. Site A2 is situated at the juncture of Sectors F2, F3, E, and G and the mean GEM concentration measured was 3.0 ng m^{-3}, which fits into interpolated GEM concentration contour from the MerPAS deployments at this location (2.80–3.23 ng m^{-3}). Similarly, the mean GEM concentration at site A3 (2.7 ng m^{-3}) is falls within the range of GEM concentrations measured at adjacent MerPAS sites P31 (2.17 ng m^{-3}) and P28 (2.87 ng m^{-3}). Although there was a four-year difference between the active and passive deployments, it appears any long-term temporal differences that might occur (i.e. landfill disturbances or changes in waste incineration plant output) had very little effect on the GEM concentrations measured by either method in these two time periods.

The WHO lists the non-occupational minimal risk level (MRL) for chronic inhalation (365 days) of GEM in Europe to be 1000 ng m^{-3} (WHO 2000). A stricter MRL of 200 ng m^{-3} is applied in the USA by the US Agency for Toxic Substances and Disease Registry (USATSDR 2016). The maximum observed passive GEM concentration was ≈100× less than this threshold value (≈20× less than the USATSDR value) and background concentrations were observed outside the Gamsenried landfill site. Hence, there is no chronic inhalation exposure risk from GEM for the local population living in the vicinity of the Gamsenried landfill site. While the active instruments measured higher GEM concentrations (still >5× lower than either chronic MRL), these

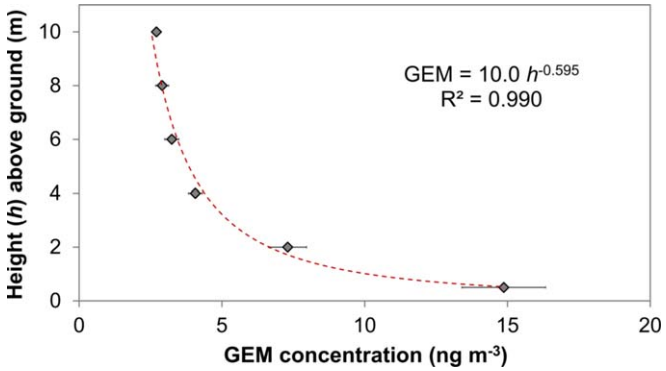

Figure 4. Vertical GEM concentration gradient measured at site 29 in landfill Sector 3. The dashed red curve indicates the power relationship between GEM concentration and height above the ground.

5-min maximum concentrations are more relevant to acute rather than chronic exposures. Acute exposures, of course, carry inherently higher threshold value for MRLs (USATSDR 2016).

The GEM concentrations measured by the MerPAS samplers outside the landfill area were 1.64, 1.63, and 1.64 ng m^{-3}, for site P1, P32, and the measurement made in the town of Visp, respectively. All three sites are essentially the same as the assessment of background concentrations made using the active instrument four summers earlier in 2016, which again agrees well with the range of background concentrations measured in the Northern Hemisphere (Sprovieri *et al* 2016). The excellent agreement between these data support suggestions made elsewhere that MerPAS is a suitable tool for monitoring GEM concentrations at both background and source areas (McLagan *et al* 2018a, 2018b, 2019).

The vertical GEM concentration gradient was assessed using duplicated MerPAS deployed at 0.5, 2, 4, 6, 8, and 10 m on a telescopic sampling tower at site 29. The mean GEM concentrations of the duplicated samplers ranged from 14.9 ng m^{-3} at 0.5 m above-ground to 2.71 ng m^{-3} at 10 m above-ground and data fit strongly ($R^2 = 0.990$) with a power relationship (figure 4). McLagan *et al* (2019) made similar vertical deployments using these samplers at a former Hg mine in Italy and determined a less 'steep' logarithmic decrease in concentration with height. Nonetheless, they utilised existing structures as the supporting substrate for MerPAS and suggested the structures themselves may have emitted some GEM and/or influenced wind patterns (McLagan *et al* 2019). The telescopic towers used here are more suited to the purpose of sampling the vertical GEM concentration gradient because (i) they were brought to the site and presumably not contaminated with GEM, and (ii) their narrow diameter (5–10 cm) would have little effect on normal wind conditions. Thus, we suggest the measured power relationship between height above the ground and GEM concentration in this study to be more appropriate than the previously determined relationship by McLagan *et al* (2019), particularly for this site.

3.3. GEM emissions estimate

Combining the mean GEM concentration from the high spatial resolution MerPAS deployment across the Gamsenried landfill site (3.45 ng m^{-3}, converted to 5.44 ng m^{-3} at 0.5 m above the ground; figure S4) with the vertical GEM concentration data we can estimate a well-mixed 3D box of homogenous GEM concentration. The height of this well-mixed box, the *equivalent height* (3.4 m), is determined by integration of the vertical GEM concentration gradient extrapolated upwards to background GEM concentration (assumed as 1.62 ng m^{-3} measured by the Tekran 2537A at site A3 during the idle period of the incineration plant in 2016). Using the mean measured horizontal wind speed (and assumed non-zero vertical wind speed of 0.01 m s^{-1}) to control the advection rate of GEM at the site, the difference between the inputs (upwind) and outputs (downwind) of GEM in the well-mixed box represent the emissions of GEM for the site. Based on these data, the emissions of GEM from the Gamsenried landfill site are 1.1 $\pm$ 0.5 kg of Hg per year (or 290 $\pm$ 140 ng m^{-2} h^{-1}). A more complex model estimation based on the respective areas and mean concentrations of each of the elevated GEM concentration contours in figure 3 was also made (see section S4 for details) and determined to be 1.6 $\pm$ 0.8 kg yr^{-1} (or 410 $\pm$ 200 ng m^{-2} h^{-1}). The geospatially interpolated GEM concentrations attempt to provide spatial continuity of data where the resolution of empirical measurements is limited (Li and Heap 2011). It is therefore likely that the kriging-based model provides an improvement in the GEM emissions estimation, particularly in cases where the spatial uniformity sampling is not equal such as at the distribution of MerPAS sampling sites at Gamsenried landfill. Moradi *et al* (2021) applied this box modelling approach to assess fugitive polycyclic aromatic compound emissions from Alberta Oil Sands tailing ponds but used a vertical wind speed of zero as it is expected over long term this will average out to zero or very close. This is a valid and supported assumption

(Weiss *et al* 2007). Applying a net zero vertical wind speed, emissions estimates are 0.56 ± 0.28 kg of Hg per year (or 150 ± 120 ng m^{-2} h^{-1}) for the simple model and 1.2 ± 0.6 kg yr^{-1} (or 310 ± 150 ng m^{-2} h^{-1}) for the more complex model. These data show the more complex model is also less sensitive to changes in the assumed vertical wind speed. We suggest the more complex, spatially balanced model with a net zero vertical wind speed to be the best method of estimate GEM emissions. Considering GEM emissions are known to increase with temperature and solar radiation (Carpi and Lindberg 1997, Poissant and Casimir 1998, Choi and Holsen 2009), the emissions estimates made from summertime measurements are likely to represent the upper range of emissions.

Annual emissions from the Gamsenried landfill are on a similar magnitude to landfill emissions from the working face in China and the USA that range from ≈0.1–3.5 kg yr^{-1} collated in a recent review by Tao *et al* (2017). The area normalised fluxes from the landfill were also in a similar range to the values (20–1392 ng m^{-2} h^{-1}) measured by Osterwalder *et al* (2019) using flux chambers from Hg polluted soils in settlement areas of Visp and Turtig-Raron (ca. 4 km west of landfill). Nonetheless, the more complex, zero vertical wind speed estimate from the Gamsenried landfill ≈70–130× less than the estimates calculated for the former Hg mine in Italy (80 ± 40 and 150 ± 75 kg yr^{-1} in autumn and summer, respectively; McLagan *et al* 2019) in which this emissions estimate method was introducted. As previously mentioned, the measured vertical gradient in that study was more uncertain and indicative of a less steep decrease in GEM concentration with height above the ground likely associated with interferences from the building structures used as the substrate to hold the samplers and the assumed 0.01 m s^{-1} vertical wind speed (McLagan *et al* 2019). If we apply the measured vertical gradient from site 29 and zero vertical wind speed to the data from the Italian Hg mine the autumn and summer emissions estimates would be 11 ± 5 and 21 ± 10 kg yr^{-1} (or 18 ± 9 and 32 ± 16 kg yr^{-1} by interpolating emissions to 0.5 m, which was not done in that study), respectively, or 14% (or 22% at 0.5 m) of the previous estimate; and hence, the original estimates are likely to overestimate emissions at that site.

The Swiss Federal office for the Environment (FOEN) list total Hg emissions from the country on the order of 670 kg of Hg per year (FOEN 2020). Recent Hg emissions inventories estimate global emissions to be ≈2 × 10^6 kg of Hg per year (Pacyna *et al* 2010, Pirrone *et al* 2010), to which contaminated sites are estimated to contribute 8.2 × 10^4 kg of Hg per year (Kocman *et al* 2013). Thus, emissions from the Gamsenried landfill represent very small contributions to annual Swiss Hg emissions and global contaminated site and total Hg emissions (≈0.2, ≈0.001, and <0.0001%, respectively).

4. Conclusions

Both the active and passively derived GEM concentrations measured at the Gamsenried landfill were elevated above background by up to 23× and 7×, respectively. These data highlight the advantages and disadvantages of both monitoring methods. The 5-min sampling resolution of the active instrument allows assessment of short-term temporal variability in GEM concentrations (i.e. diurnal or daily variability) that cannot be made with the passive samplers that provide concentrations averaged across the whole time they are deployed. While minimum deployment times of passive samplers are dependent upon ambient GEM concentration and can be substantially reduced in highly contaminated environments (>1000 ng m^{-3}) to potentially hourly deployments (McLagan *et al* 2019), this requires considerable increase in asset (sampler), time (around the clock deployments and collections), and analytical demands that likely renders such passive sampler deployments for more than a day or two unfeasible. Nonetheless, MerPAS has a distinct advantage in characterizing spatial variability in concentrations that cannot be achieved with active instruments whose mobility is limited by their power (and carrier gas for certain instruments) requirements. This extends to assessments of vertical gradients, which, using the telescopic tower applied in this study, generated an improved (lower uncertainty) power relationship between GEM concentration and height above ground. These high spatial resolution horizontal and vertical MerPAS deployments were modelled to produce an emissions estimate of 1.2 ± 0.6 kg yr^{-1} (or 310 ± 150 ng m^{-2} h^{-1}) based on a method that accounts for spatial heterogeneity of sampling sites and a net zero average vertical wind speed. This study highlights the benefits of combining both active and passive sampling methods to holistically gauge spatial and temporal variability in GEM concentrations and emissions to the atmosphere from legacy sites contaminated by Hg.

Acknowledgments

The authors would like to thank the Lonza AG team at the Gamsenried landfill for their assistance with the active and passive sampling on site: Anton Aeby, Helmut Imboden, and Markus Juon. The Atmospheric Sciences group of the University of Basel is acknowledged for providing the mobile weather station. We also acknowledge Thibault Rohner and Remo Schweiger for assistance during setup of the active sampling system on the landfill.

We thank the Federal Office of Meteorology and Climatology MeteoSwiss for providing data from the Visp (VIS) meteorological station. The authors also acknowledge funding for the project that was provided by Lonza AG.

Data availability statement

All data that support the findings of this study are included within the article (and any supplementary files).

Conflicts of interest

Tekran Instruments Corp. pays some licensing fees to the University of Toronto related to the sale of MerPAS, which is in part distributed to D S M.

ORCID iDs

David S McLagan https://orcid.org/0000-0003-2586-625X

References

Agnan Y, Le Dantec T, Moore C, Edwards G C and Obrist D 2016 New constraints on terrestrial surface–atmosphere fluxes of gaseous elemental mercury using a global database *Environ. Sci. Technol.* **50** 507–24

Aspmo K, Gauchard P-A, Steffen A, Temme C, Berg T, Bahlmann E, Banic C, Dommergue A, Ebinghaus R and Ferrari C 2005 Measurements of atmospheric mercury species during an international study of mercury depletion events at NyÅlesund, Svalbard, spring 2003 How reproducible are our present methods? *Atmos. Environ.* **39** 7607–19

Biester H 2020 *Verteilung, Speziation und Mobilität von Quecksilber Deponie Gamsenried Lonza AG Visp Phase DUB2 Etappe 1 und Etappe 2* Technische Universität Braunschweig and Lonza AG 1–84

Carmona M, Llanos W, Higueras P and Kocman D 2013 Mercury emissions in equilibrium: a novel approach for the quantification of mercury emissions from contaminated soils *Anal. Methods* **5** 2793–801

Carpi A and Lindberg S E 1997 sunlight-mediated emission of elemental mercury from soil amended with municipal sewage sludge *Environ. Sci. Technol.* **31** 2085–91

Choi H - D and Holsen T M 2009 Gaseous mercury emissions from unsterilized and sterilized soils: the effect of temperature and UV radiation *Environ. Poll.* **157** 1673–8

Driscoll C T, Mason R P, Chan H M, Jacob D J and Pirrone N 2013 Mercury as a global pollutant: sources, pathways, and effects *Environ. Sci. Technol.* **47** 4967–83

Edwards G C, Rasmussen P E, Schroeder W H, Kemp R J, Dias G M, Fitzgerald-Hubble C R, Wong E K, Halfpenny-Mitchell L and Gustin M S 2001 Sources of variability in mercury flux measurements *J. Geophys. Res. Atmos.* **106** 5421–35

Engle M, Gustin M S and Zhang H 2001 Quantifying natural source mercury emissions from the Ivanhoe mining district, north-central Nevada, USA *Atmos. Environ.* **35** 3987–97

Engle M A, Tate M T, Krabbenhoft D P, Schauer J J, Kolker A, Shanley J B and Bothner M H 2010 Comparison of atmospheric mercury speciation and deposition at nine sites across central and eastern North America *J. Geophys. Res. Atmos.* **115** D18

Ferrara R, Mazzolai B, Edner H, Svanberg S and Wallinder E 1998 Atmospheric mercury sources in the Mt Amiata area, Italy *Sci. Tot. Environ.* **213** 13–23

FOEN 2020 *Switzerland's Informative Inventory Report 2020 (IIR): Submission under the UNECE Convention on Long-Range Transboundary Air Pollution: Submission of March 2020* United Nations ECE Secretariat Federal Office for the Environment (FOEN) Air Pollution Control and Chemicals Division 1–374 Bern, Switzerland https://bafu.admin.ch/dam/bafu/de/dokumente/luft/fachinfo-daten/Switzerlands-Informative-Inventory-Report-2019.pdf.download.pdf/switzerlands-informative-rep-2020.pdf

Gustin M S, Biester H and Kim C S 2002 Investigation of the light-enhanced emission of mercury from naturally enriched substrates *Atmos. Environ.* **36** 3241–54

Jeon B, Cizdziel J V, Brewer J S, Luke W T, Cohen M D, Ren X and Kelley P 2020 Gaseous elemental mercury concentrations along the northern Gulf of Mexico using passive air sampling, with a comparison to active sampling *Atmos.* **11** 1034

Kocman D and Horvat M 2011 Non-point source mercury emission from the Idrija Hg-mine region: GIS mercury emission model *J. Environ. Manage.* **92** 2038–46

Kocman D, Horvat M, Pirrone N and Cinnirella S 2013 Contribution of contaminated sites to the global mercury budget *Environ. Res.* **125** 160–70

Li J and Heap A D 2011 A review of comparative studies of spatial interpolation methods in environmental sciences: performance and impact factors *Ecol. Inform.* **6** 228–41

Lyman S N and Gustin M S 2008 Speciation of atmospheric mercury at two sites in northern Nevada, USA *Atmos. Environ.* **42** 927–39

McLagan D S, Huang H, Lei Y D, Wania F and Mitchell C P J 2017a Application of sodium carbonate prevents sulphur poisoning of catalysts in automated total mercury analysis *Spectrochim. Acta B* **133** 60–2

McLagan D S, Mitchell C P J, Huang H, Abdul Hussain B, Lei Y D and Wania F 2017b The effects of meteorological parameters and diffusive barrier reuse on the sampling rate of a passive air sampler for gaseous mercury *Atmos. Meas. Tech.* **10** 3651–60

McLagan D S *et al* 2018a Global evaluation and calibration of a passive air sampler for gaseous mercury *Atmos. Chem. Phys.* **18** 5905–19

McLagan D S, Abdul Hussain B, Huang H, Lei Y D, Wania F and Mitchell C P J 2018b Identifying and evaluating urban mercury emission sources through passive sampler-based mapping of atmospheric concentrations *Environ. Res. Lett.* **13** 074008

McLagan D S, Monaci F, Huang H, Lei Y D, Mitchell C P J and Wania F 2019 Characterization and quantification of atmospheric mercury sources using passive air *J. Geophys. Res. Atmos.* **124** 2351–62

Moradi M, You Y, Hung H, Li J, Park R, Alexandrou N, Moussa S G, Jantunen L, Robitaille R and Staebler R M 2021 Fugitive emissions of polycyclic aromatic compounds from an oil sands tailings pond based on fugacity and inverse dispersion flux calculations *Environ. Poll.* **269** 116115

Naccarato A *et al* 2020 A field intercomparison of three passive air samplers for gaseous mercury in ambient air *Atmos. Meas. Tech. Discussion* 1–34

O'Connor D, Hou D, Ok Y S, Mulder J, Duan L, Wu Q, Wang S, Tack F M G and Rinklebe J 2019 Mercury speciation, transformation, and transportation in soils, atmospheric flux, and implications for risk management: a critical review *Environ. Int.* **126** 747–61

Osterwalder S, Huang J H, Shetaya W H, Agnan Y, Frossard A, Frey B and Obrist D 2019 Mercury emission from industrially contaminated soils in relation to chemical, microbial, and meteorological factors *Environ. Poll.* **250** 944–52

Pacyna E G, Pacyna J M, Sundseth K, Munthe J, Kindbom K, Wilson S, Steenhuisen F and Maxson P 2010 Global emission of mercury to the atmosphere from anthropogenic sources in 2005 and projections to 2020 *Atmos. Environ.* **44** 2487–99

Pirrone N *et al* 2010 Global mercury emissions to the atmosphere from anthropogenic and natural sources *Atmos. Chem. Phys.* **10** 5951–64

Poissant L and Casimir A 1998 Water-air and soil-air exchange rate of total gaseous mercury measured at background sites *Atmos. Environ.* **32** 883–93

Song S *et al* 2015 Top-down constraints on atmospheric mercury emissions and implications for global biogeochemical cycling *Atmos. Chem. Phys.* **15** 7103–25

Sprovieri F, Pirrone N, Bencardino M, D'Amore F, Carbone F, Cinnirella S and Brunke E G 2016 Atmospheric mercury concentrations observed at ground-based monitoring sites globally distributed in the framework of the GMOS network *Atmos. Chem. Phys.* **16** 11915

Steinmann B 2016 *Ergänzende historische Untersuchung der alten Deponie Gamsenried interner Bericht* Lonza AG Visp, Switzerland

Streets D G, Horowitz H M, Jacob D J, Lu Z, Levin L, Ter Schure A F and Sunderland E M 2017 Total mercury released to the environment by human activities *Environ. Sci. Technol.* **51** 5969–77

Szponar N, McLagan D S, Kaplan R J, Mitchell C P J, Wania F, Steffen A and Bergquist B A 2020 Isotopic characterization of atmospheric gaseous elemental mercury by passive air sampling *Environ. Sci. Technol.* **54** 10533–43

Tao Z, Dai S and Chai X 2017 Mercury emission to the atmosphere from municipal solid waste landfills: a brief review *Atmos. Environ.* **170** 303–11

Temme C, Blanchard P, Steffen A, Banic C, Beauchamp S, Poissant L, Tordon R and Wiens B 2007 Trend, seasonal and multivariate analysis study of total gaseous mercury data from the Canadian atmospheric mercury measurement network (CAMNet) *Atmos. Environ.* **41** 5423–41

UNEP 2013 *Minamata convention on mercury: Text and annexes* United Nations Environmental Programme (UNEP) 1–67 Geneva, Switzerland http://hdl.handle.net/20.500.11822/8541)

USATSDR 2021 *Minimal risk levels May 2021* United States Agency for Toxic Substances and Disease Registry (USATSDR) 1–17 Atlanta, USA https://wwwn.cdc.gov/TSP/MRLS/mrlsListing.aspx

Wang S, Feng X, Qiu G, Fu X, Wei Z and Xiao T 2005 Mercury emission to atmosphere from Lanmuchang Hg–Tl mining area, South western Guizhou, China *Atmos. Environ.* **39** 7459–73

Weiss A, Kuss J, Peters G and Schneider B 2007 Evaluating transfer velocity-wind speed relationship using a long-term series of direct eddy correlation CO_2 flux measurements *J. Mar. Syst.* **66** 130–9

WHO 2000 *Air Quality Guidelines For Europe* World Health Organisation (WHO) Regional Office for Europe 1–273 Copenhagen, Denmark https://euro.who.int/__data/assets/pdf_file/0005/74732/E71922.pdf

Wohlgemuth L, McLagan D, Flückiger B, Vienneau D and Osterwalder S 2020 Concurrently measured concentrations of atmospheric mercury in indoor (household) and outdoor air of basel, Switzerland *Environ. Sci. Technol. Lett.* **7** 234–9

Zhu W, Sommar J, Lin C J and Feng X 2015 Mercury vapor air–surface exchange measured by collocated micrometeorological and enclosure methods–Part I: data comparability and method characteristics *Atmos. Chem. Phys.* **15** 685–702